Expression of Phosphatidylinositol (4,5) Bisphosphate–specific Pleckstrin Homology Domains Alters Direction But Not the Level of Axonal Transport of Mitochondria[D]

Kurt J. De Vos,* Julia Sable, Kyle E. Miller, and Michael P. Sheetz,[†]

*Department of Biological Sciences, Columbia University, New York, New York 10027

Axonal transport of membranous organelles such as mitochondria is essential for neuron viability and function. How signaling mechanisms regulate or influence mitochondrial distribution and transport is still largely unknown. We observed an increase in the distal distribution of mitochondria in neurons upon the expression of pleckstrin homology (PH) domains of phospholipase Cδ1 (PLCδ-PH) and spectrin (spectrin-PH). Quantitative analysis of mitochondrial transport showed that specific binding of PH domains to phosphatidylinositol (4,5) bisphosphate (PtdIns(4,5)P2) but not 3' phosphorylated phosphatidylinositol species enhanced plus-end–directed transport of mitochondria two- to threefold and at the same time decreased minus-end–directed transport of mitochondria along axonal microtubules (MTs) without altering the overall level of motility. Further, the velocity and duration of mitochondrial transport plus the association of molecular motors with mitochondria remained unchanged by the expression of PH domains. Thus, PtdIns(4,5)P2-specific PH domains caused an increase in distal mitochondria by disturbing the balance of plus- and minus-end–directed transport rather than directly affecting the molecular machinery involved. Taken together our data reveal that level and directionality of transport are separable and that PtdIns(4,5)P2 has a novel role in regulation of the directionality of axonal transport of mitochondria.

INTRODUCTION

Mitochondria are the main energy providers in virtually all mammalian cells and are the site of numerous biosynthetic and degradative pathways that are essential for cell function. The distribution of mitochondria is thought to be controlled by local energy and metabolic demand. Maintaining

sufficient energy and metabolic supply to all cellular regions becomes exceedingly difficult in large, highly polarized cells such as neurons. Consequently, an efficient control of mitochondrial distribution and transport in response to cellular processes and stimuli is essential for neuronal development and survival.

All components of the cytoskeleton, MTs, actin microfilaments, and intermediate filaments, have been implicated in transport and positioning of mitochondria. After the discovery of molecular motors such as kinesin and cytoplasmic dynein, it became clear that mitochondria are transported bidirectionally over long distances along MTs by molecular motors (Leopold *et al.,* 1992; Rodionov *et al.,* 1993; Jellali *et al.,* 1994; Tanaka *et al.,* 1998). This long-distance transport constitutes a major mechanism in establishing the dispersal of mitochondria in the cytoplasm. Additionally, unconventional myosin-based transport along actin filaments was implicated in mitochondrial transport, but, actin-based transport does not seem to cover long distances (Morris and Hollenbeck, 1995; Ligon and Steward, 2000). Possibly actin-based transport optimizes mitochondrial localization after MT-based transport. Lastly, intermediate filaments might also be involved in mitochondrial motility and distribution, perhaps by anchoring mitochondria in place during station-

ary periods (Toh *et al.,* 1980; Reipert *et al.,* 1999; Milner *et al.,* 2000; Linden *et al.,* 2001).

Several mechanisms were proposed to regulate kinesin- and cytoplasmic dynein-based transport, including conformational changes and phosphorylation. Alternatively, MT-associated proteins such as tau, MAP2, and MAP4 can indirectly block MT-based transport, most likely by steric hindrance and/or by competition for MT binding (for review see Sheetz, 1999; Reilein *et al.,* 2001). It was reported that phosphorylation of kinesin light chain (KLC) inhibits plus-end–directed movement of mitochondria at the onset of tumor necrosis factor–induced cell death (De Vos *et al.,* 2000), which could be related to GSK3 inactivation of conventional kinesin-based transport by phosphorylation of KLC (Morfini *et al.,* 2002). However, it is not clear which signaling pathways regulate mitochondrial transport.

Phosphorylated phosphatidylinositols (PtdInsPs) have been implicated in a variety of membrane transport processes such as plasma membrane-endosome recycling, phagocytosis, and MT-based transport of axonal vesicles (Vallis *et al.,* 1999; Botelho *et al.,* 2000; Brown *et al.,* 2001; Muresan *et al.,* 2001). In the case of cytoplasmic dynein-mediated transport, it was proposed that PtdIns(4,5)P2 serves as binding site for spectrin, which in turn interacts with the ARP1 component of the cytoplasmic dynein-activating complex dynactin, thus allowing cytoplasmic dynein to bind to its membranous cargo (Muresan *et al.,* 2001). It was reported that the mitochondria contain PtdInsPs and bind spectrin, but it is not known if these components play a role in interaction of molecular motors with mitochondria (Seyfred and Wells, 1984; Zagon *et al.,* 1986; Bothmer *et al.,* 1992; Tran *et al.,* 1993). In addition, the plus-end–directed molecular motor Unc104 binds directly to PtdIns(4,5)P2 through its PH domain and clustering of Unc104 in PtdIns(4,5)P2-containing rafts provides a trigger for membrane transport (Klopfenstein *et al.,* 2002). However, no known mitochondrial motor has a similar lipid-binding domain.

Here we report that specific binding of PH domains to PtdIns(4,5)P2, but not 3′ phosphorylated PtdInsPs in vivo increases plus-end–directed transport and at the same time decreases minus-end–directed transport of mitochondria along MTs, without affecting total transport levels. Velocity and duration of remaining minus-end–directed transport and of plus-end–directed transport are not affected by binding PtdIns(4,5)P2, and association of conventional kinesin or cytoplasmic dynein with mitochondria is not altered by expression of PH domains, indicating that PtdIns(4,5)P2-dependent regulation of molecular motor activity rather than mitochondria-motor interaction is at the basis of these observations. Taken together we propose a role for PtdIns(4,5)P2-dependent signaling pathways in the regulation of the balance between plus- and minus-end–directed mitochondrial transport and distribution in axons.

MATERIALS AND METHODS

Cell Culture and Transfection

N2A neuroblastoma cells and derived clones were maintained in Dulbecco's modified Eagle's medium (DMEM) supplemented with 10% fetal calf serum, 2 mM L-glutamine, 4 mM sodium pyruvate, 200 U/ml streptomycin, and 100 U/ml penicillin (all from Invitrogen, Carlsbad, CA). Transfections, stable and transient, were performed using Lipofectamine Plus reagents (GibcoBRL) or ExGen500 (MBI-Fermentas, Hanover, MD) according to the manufacturer's protocol.

For differentiation N2A cells were transferred to DMEM containing N2 supplement (GibcoBRL), 2 mM L-glutamine, 4 mM sodium pyruvate, 200 U/ml streptomycin, and 100 U/ml penicillin for at least 24 h. We selected the processes to analyze based on their length; axons are significantly longer than neurites in these cells (Yu *et al.,* 1997), and their morphology, in particular the transition from cell body to process, is better defined in the case of axon-like processes. The processes formed under these differentiation conditions that match those criteria are positive for the microtubule binding protein tau (present in both axons and neurites) and negative for the neurite-specific microtubule-binding protein MAP2, confirming they are axon-like (supplementary Figure 1).

Plasmids

Mitochondria were labeled with red fluorescent protein using pD-sRed1-Mito (Clontech, Palo Alto, CA). EGFP-tagged PH domain of PLCδ was a generous gift of Dr T. Meyer (Duke University; Stauffer *et al.,* 1998). The EGFP-tagged PH domain of spectrin was derived from βG-spectrin (a kind gift of Dr. V Bennett, Duke University; Davis and Bennett, 1994). The PH domain (AA 2197–2307) was excised from βG-5.1 spectrin cDNA by digest with *Sal*I and *Hind*III at the NH2 and COOH terminals, respectively, and was subcloned into pEGFP-C1 (Clontech) using P1-GCGCAAGCTTCGTCGGC-CCAGATGGAAGCC and P2-GCGCGTCGACGGAGATGGCG-GAAGAGATAGC as primers. EGFP-tagged PH domain of general receptor of phosphoinositides 1 (GRP1) was a kind gift of Dr. M. A. Lemmon (University of Pennsylvania, Philadelphia, PA) and was described previously (Kavran *et al.,* 1998). H6-PLCδ-PH-EGFP used for in vitro studies was a gift of Dr. S. Scarlata (SUNY Stony Brook; Wang *et al.,* 1999).

Quantitative Analysis of Mitochondrial Motility

Image analysis was done with the open source image analysis programs ImageJ (by W. Rasband (NIH, Bethseda, MD; http://rsb.info.nih.gov/ImageJ) and Object Image (by N. Visscher (University of Amsterdam, The Netherlands, http://simon.bio.uva.nl) using available and custom made plugins and macros,and with PhotoShop (Adobe Systems, San Jose, CA).

We developed a semiautomated tracking routine in Object Image, which allowed us to follow up to 200 mitochondria per cell simultaneously over time. The cells were transfected with DsRed1-Mito to visualize the mitochondria. The position of the mitochondria was recorded by time-lapse fluorescence microscopy (3-s interval). The time stacks were imported in Object Image and the x and y coordinates of the centroid of mitochondrial fluorescence was determined for all mitochondria at each time point (see Figure 4A).

By defining a fixed reference point (the centroid of the nucleus), the distance of the mitochondria to the center of the nucleus was computed. Because of the highly organized architecture of the MT array in axons with the plus ends pointing away from the cell body toward the growth cone, we could include directional information in the analysis (practically, if the distance from the reference point increases, there is plus-end–directed movement; if the distance decreases, there is minus-end–directed movement).

Mitochondrial motility was expressed in terms of the net displacement, frequency, velocity, and duration of movements in either the plus- or the minus-end direction. Additionally, we determined the motility profile per mitochondrion.

First, we determined the velocities per mitochondrium for each time point by calculating the distance each mitochondrium moved relative to its position at the previous time point and dividing this distance by the time elapsed per frame (this yields a positive veloc-

ity for movement toward growth cone, and a negative velocity for movement toward the cell body). We applied a threshold of absolute velocities of 300 nm/s, which is two times the spatial resolution of the recorded images to define motility events, discriminating plus- and minus-end–directed events. Plus- and minus-end–directed events were treated separately in the following calculations. Tallying the number of these events per second and per mitochondrion results in the frequency of movement. The velocities of all plus- or minus-end–directed events were averaged to yield the average velocity. The duration of movement was defined as the period of an ongoing transport in one direction without halting or reversal of direction.

For analysis of the motility profile of mitochondria we quantified plus-e and minus-end–directed motility for all axonal mitochondria individually by tallying plus- and minus-end–directed motility events. Subsequently, the relative percentage of plus- and minus-end–directed events were calculated, and a motility histogram was constructed, showing the motility behavior of individual mitochondria (see Figure 5A).

Indirect Immunofluorescence of Isolated Mitochondria

N2A cells were harvested by trypsinization, transferred to 4°C, and washed twice with ice-cold PBS and once with ice cold I-buffer (100 mM K-HEPES, 220 mM mannitol, 70 mM sucrose, 1 mM EDTA, 1 mM DTT, and 1 mM PMSF, pH 7.4). The cell pellet (800 × *g*, 10 min, 4°C) was resuspended in 0.9 volumes of I-buffer and homogenized with a tissue grinder (pestle 19, 100 strokes, Kontes, Vineland, NJ) or ball-bearing cell breaker (10 strokes). Unbroken cells and nuclei were removed by centrifugation (3000 × *g*, 10 min, 4°C). A crude mitochondrial pellet was obtained by centrifugation of the remaining supernatant for 15 min at 13,000 × *g*. Resuspended mitochondria were incubated with 1 μg/ml antikinesin mAb SUK4 (Ingold *et al.,* 1988) or anticytoplasmic dynein IC mAb (1/100, Chemicon, Temecula, CA) in I-buffer followed by Alexa 647–labeled goat anti-mouse Ig polyclonal antibody (antibody; 1/500; Molecular Probes, Eugene, OR). Subsequently, stained mitochondria were observed using a Fluoview confocal microscope (Olympus, Melville, NY). Mitochondria from transfected cells were identified by transfection with DsRed1-Mito (Clontech).

Competition Assay

Mitochondria were isolated over a discontinuous sucrose gradient as described before (De Vos *et al.,* 2000). Isolated mitochondria were incubated with 10 μg purified PLCδ-PH or 10 μM MARCKS effector domain peptide for 30 min at room temperature. After extensive washing mitochondria were lysed in Laemmli sample buffer and separated on 7.5% SDS-PAGE. Proteins were blotted to nitrocellulose membranes (Optitran; Schleicher & Schuell, Keene, NH) and processed for Western blotting. Conventional kinesin was detected using anti-KIF5B antibody (a generous gift of Dr. R. Vale, UCSF) followed by HRP-coupled anti-rabbit IgG(H+L) antibody (Jackson ImmunoResearch Laboratories, West Grove, PA); cytoplasmic dynein was probed with antidynein IC 74 mAb (Chemicon) and HRP-coupled anti-mouse IgG antibody (Amersham, Piscatawy, NJ). ECL (Amersham) detection was performed according to the manufacturer's protocol.

MT Affinity Assay

High-speed cytosol was obtained by breaking N2A cells in ice-cold BRB80 (80 mM K-PIPES, 1 mM MgCl$_2$, 1 mM EGTA, pH 6.8) supplemented with protease inhibitors (Complete, Roche Diagnostics, Indianapolis, IN) followed by centrifugation (100,000 × *g*, 30 min, 4°C). High-speed cytosol was adjusted to 5 mg/ml and supplemented with 50 μl Taxol-stabilized MTs (2 mg/ml), 1 mM AMP-PNP, 1 mM GTP, and 10 μM Taxol and incubated for 20 min at room temperature. Taxol-stabilized MTs and associated proteins were subsequently separated from nonassociated cytosolic proteins by centrifugation over a 60% vol/vol glycerol BRB80 cushion (200,000 × *g*, 2 h, 20°C), and resuspended in Laemmli loading buffer. The proteins were separated on 7.5% SDS-PAGE and detected by Commassie-R250 staining (Bio-Rad, Hercules, CA).

RESULTS

PtdIns(4,5)P2-specific PH Domains Cause Accumulation of Mitochondria But Not Endosomes in Axons

PH domains were identified in a variety of proteins and bind to the polar headgroup of PtdInsPs with high affinity. When ectopically expressed in cells, PH domains specifically bind their counterpart PtdInsPs and consequently influence PtdInsP-dependent cellular processes (Holz *et al.,* 2000; Raucher *et al.,* 2000). Importantly, the specificity of distinct PH domains for different PtdInsPs makes it possible to discriminate between the effect of several different forms of PtdInsP on one given process, making them powerful tools to study involvement of PtdInsPs in cellular processes (Davis and Bennett, 1994; Garcia *et al.,* 1995; Rameh *et al.,* 1997; Kavran *et al.,* 1998; Holz *et al.,* 2000; Klarlund *et al.,* 2000).

To evaluate a possible involvement of PtdInsPs in the control of organelle motility and distribution in neurons, we expressed the PH domains of PLCδ (PLCδ-PH), spectrin (spectrin-PH), and GRP1 (GRP1-PH) in N2A neuroblastoma cells. Although PLCδ-PH and spectrin-PH specifically bind to PtdIns(4,5)P2, GRP1-PH specifically binds to 3′ phosphorylated PtdInsPs, especially phosphatidylinositol (3,4,5) trisphosphate (PtdIns(3,4,5)P3; Davis and Bennett, 1994; Garcia *et al.,* 1995; Rameh *et al.,* 1997; Kavran *et al.,* 1998; Holz *et al.,* 2000; Klarlund *et al.,* 2000). N2A cells were differentiated to a neuronal phenotype by serum-starvation in the presence of N2-supplement. It was reported before that N2A cells put out both axon and dendrite-like processes in culture (Ross *et al.,* 1975; Yu *et al.,* 1997). Usually axon-like processes are significantly longer (~100 μm) than dendrite-like processes (~40 μm). Furthermore, the process-cell body interface is much more pronounced in the case of axon-like processes. To verify the nature of the N2A processes under these circumstances, they were stained for the microtubule-interacting proteins MAP2 and tau. Although MAP2 is exclusively found in dendrites, tau is found in axons and dendrites. Processes put out by N2A cells upon serum starvation that match length and cell body-process interface criteria, did not contain MAP2 but did contain tau, strongly suggesting they are indeed axon-like (supplementary Figure 1A). Expression of PH domains did not change the nature of the processes (supplementary Figure 1B).

In agreement with the plasma membrane localization of most of the cellular PtdIns(4,5)P2 pool (Helms *et al.,* 1991; Tran *et al.,* 1993; Watt *et al.,* 2002) PLCδ-PH was concentrated in patches at the plasma membrane relative to cytoplasm as shown by fluorescence microscopy of the EGFP tag (Figure 1). Spectrin-PH and GRP1-PH were primarily in cytoplasm although local concentrations at the plasma membrane were sometimes detected (Figure 1).

Cotransfection with DsRed1-Mito was used to follow mitochondrial distribution in the axons of N2A cells. In un-
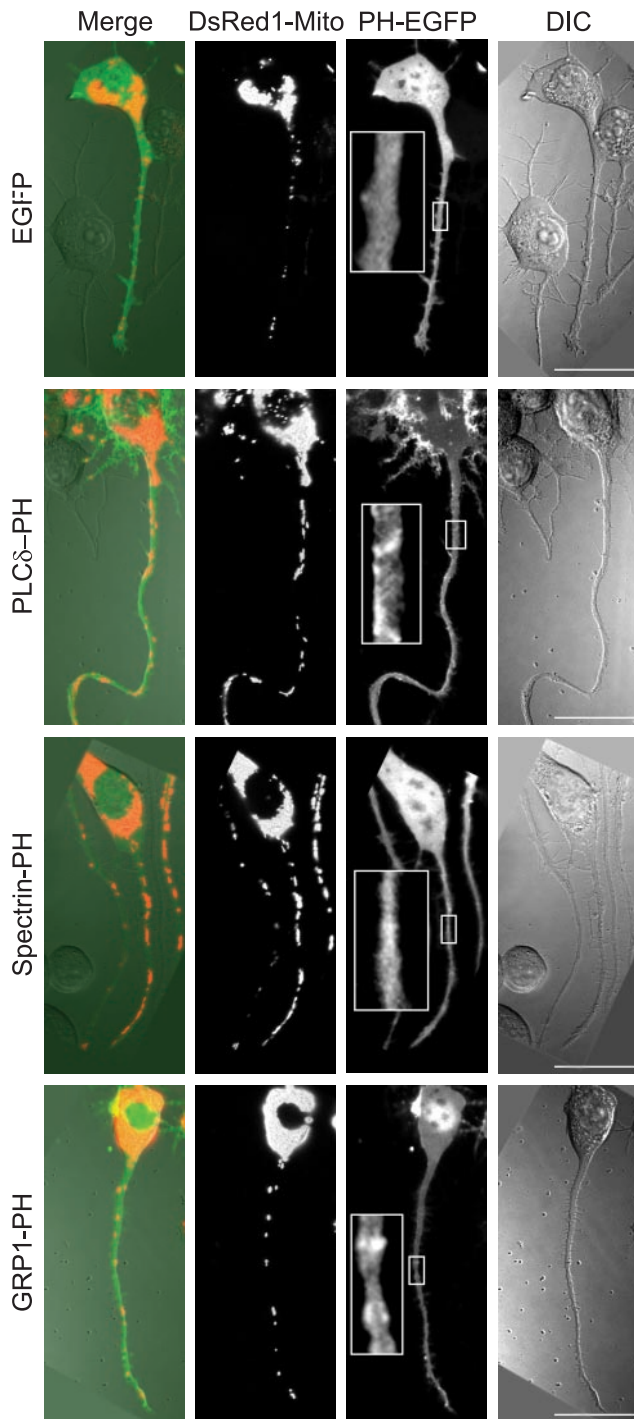
Figure 1. Distribution of mitochondria in N2A cells expressing PH domains. N2A cells were cotransfected with DsRed1-Mito and EGFP, EGFP-tagged PLCδ-PH, spectrin-PH, or GRP1-PH. The distribution of mitochondria (DsRed1-Mito) and EGFP (PH-EGFP) was determined by fluorescence microscopy. The morphology of the cells is shown by differential interference contrast (DIC). Merge: overlay of EGFP (green), mitochondria (red), and DIC (gray). Scale bar, 20 μm.

transfected and EGFP-transfected cells, axonal mitochondria resided mainly in clusters of multiple mitochondria, which were positioned along the axon at fairly constant intervals and in the growth cone (Figures 1 and 2A), consistent with efficient supply of ATP and metabolites along the length of the axon. Qualitatively, axons from PLCδ-PH and spectrin-PH-=expressing cells seemed to contain more mitochondria and/or larger clusters of mitochondria compared with axons of control cells (Figures 1 and 2A). Often, but not always, mitochondria were particularly concentrated at the distal end of the axon (i.e., at the growth cone; Figure 2A).

To evaluate the mitochondrial distribution quantitatively, we divided axons in three equal parts and determined the number of mitochondria in each subdivision. Figure 2B shows mitochondria were nearly equally dispersed in control N2A axons and axons of cells expressing GRP1-PH. In contrast, in N2A cells expressing PLCδ-PH or spectrin-PH there was a significant accumulation in the distal one third of the axon, i.e., at the growth cone (Figure 2B).

To evaluate if PtdIns(4,5)P2-specific PH domains specifically influence the distribution of mitochondria in axons, we additionally quantified the distribution of endosomes, stained with FM4–64 in PH domain-expressing N2A cells. None of the expressed PH domains influenced endosome distribution, indicating that PtdIns(4,5)P2 was involved in control of mitochondrial but not endosomal distribution in axon-like processes of N2A cells (supplementary Figure 2).

To establish the generality of this observation, we further analyzed the distribution of mitochondria and other organelles in the fibroblast cell line CV1. We did not find a change in mitochondrial, endosome, or lysosomes distribution upon expression of PH domains, indicating neuronal specificity (supplementary Figure 3).

PtdIns(4,5)P2-specific PH Domains Enhance Net Mitochondrial Transport toward the Growth Cone

Active transport of mitochondria by MT-based motors constitutes the major mechanism of redistribution over long distances (Leopold *et al.,* 1992; Jellali *et al.,* 1994; Nangaku *et al.,* 1994; Khodjakov *et al.,* 1998; Tanaka *et al.,* 1998). To dissect the involvement of mitochondrial transport in the accumulation of mitochondria after PH domain expression, we analyzed the net displacements of individual mitochondria in axons of control and PH domain-transfected cells.

Net displacement of mitochondria was defined by comparing the position of each mitochondrion before and after 15 min of time-lapse recording. We applied an empirically determined, absolute displacement threshold of 4 μm to eliminate artificial net displacement due to occasional drift of the microscope table during the time-lapse recordings (Figure 3A).

In control N2A cells, 57% of axonal mitochondria showed significant net displacement over a 15-min time span (i.e., motile mitochondria). About half (53 ± 8.35%) of these motile mitochondria showed a net displacement toward the cell body, whereas 47 ± 8.3% relocated toward the growth cone (Figure 3B). Thus, in the axon of N2A cells, constitutive transport of mitochondria was balanced.

In N2A cells expressing PLCδ-PH, the fraction of mitochondria that were displaced increased by 18–75%. Notably, only 11% of these motile mitochondria made a net movement toward the cell body, whereas 89% traveled toward the
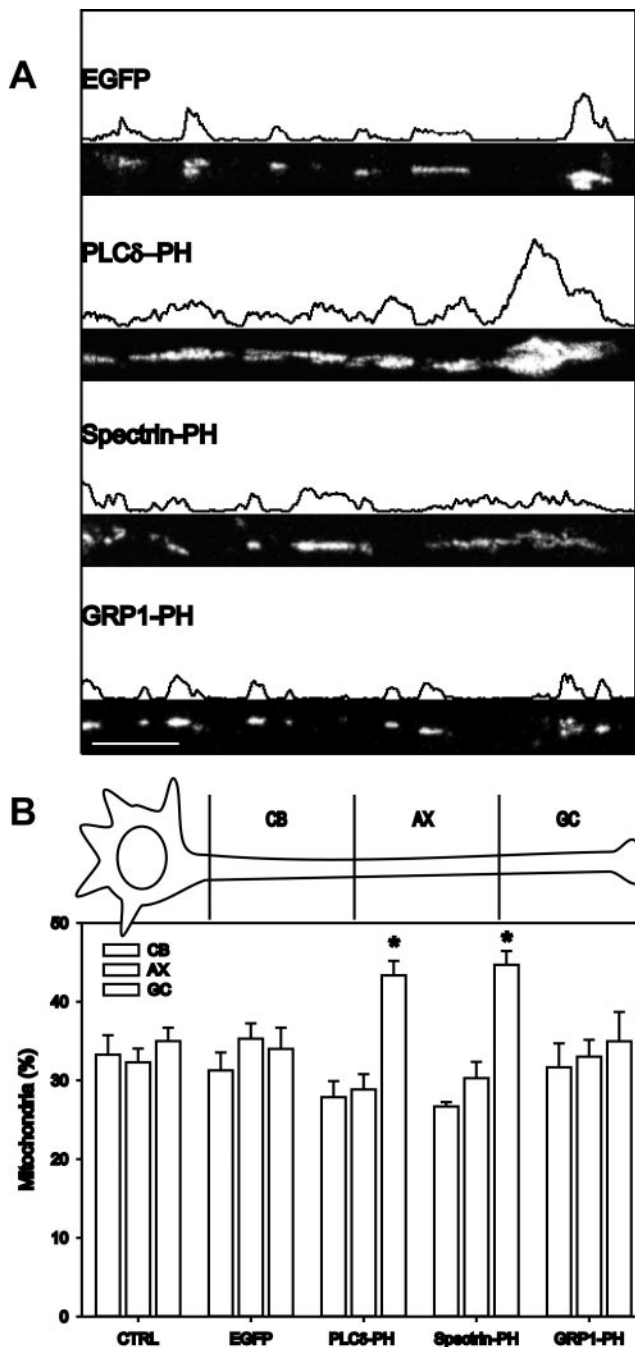
Figure 2. PtdIns(4,5)P2-specific PH domains cause distal accumulation of mitochondria. Mitochondria in the axon of cells transfected with EGFP, PLCδ-PH, spectrin-PH, or GRP1-PH were visualized by fluorescence microscopy of DsRed1-Mito. (A) Representative fluorescence images showing the distribution of axonal mitochondria and the corresponding fluorescence profile are presented. Scale bar, 20 μm. (B) The axon was divided in three equal parts ranging from the cell body (CB), over the middle of the axon (AX) to the distal part at the growth cone (GC), and the number of mitochondria in each part was determined. Data shown are the mean and SEM of at least five cells and three independent experiments per condition, *p < 0.05 (*t* test).

growth cone (Figure 3B). Spectrin-PH did not change the amount of mitochondria showing net displacement. However, the percentage of motile mitochondria that moved toward the growth cone increased, whereas the number of net displacements toward the cell body significantly decreased (Figure 3B). The effectiveness of different PH domains in altering the direction of mitochondrial motility correlated with affinities of the PH domains for PtdIns(4,5)P2: PLCδ-PH: K_D ~1 μM (Rebecchi *et al.*, 1992) and spectrin-PH: K_D ~30–50 μM (Harlan *et al.*, 1994). Finally, in agreement with the observations at the cellular level (Figures 1 and 2), we found that binding 3′ phosphorylated PtdInsPs with GRP1-PH had no significant effect on the net displacements of individual mitochondria in N2A axons (Figure 3B). Clearly, binding of PtdIns(4,5)P2 with PLCδ-PH or spectrin-PH decreased transport toward the cell body in favor of growth cone-directed transport, hence disturbing the balance of mitochondrial transport considerably.

Comparing the average length of these net displacements, we found that PH domains did not alter the distance mitochondria traveled toward the cell body or growth cone (Figure 3C), indicating that the molecular machinery driving movements was unaffected by the different treatments.

PtdIns(4,5)P2-specific PH Domains Modulate the Balance between Plus-end– and Minus-end–directed MT-based Transport of Mitochondria

Because analysis of net displacements is largely limited to unidirectional moving mitochondria and to further examine the transport activities underlying net mitochondrial displacement, we broke down the net displacements of axonal mitochondria into discrete transport events. We determined the position of all DsRed1-Mito–tagged mitochondria at each time point (15-min total recording; 3-s interval; Figure 4, A and B). From this position information, we determined the mitochondrial transport rate between frames (frequency). A velocity threshold (300 nm/s, i.e., 2 times the spatial resolution of the recorded images) was applied to define motile events. This threshold was set to include only MT-based transport of mitochondria, because the reported velocity of actin-based transport of axonal mitochondria was well below 300 nm/s (D'Andrea *et al.*, 1994; Krendel *et al.*, 1998).

Analysis of the frequency of transport in control cells revealed that the average fraction of time spent moving (plus- and minus-end–directed movements combined) was only 0.48% of the total. In other words, >99.5% of the time mitochondria remained stationary and the observed net displacements were the result of short bursts of rapid, directed transport. Nevertheless, tallying the number of mitochondria that made at least one plus-end–directed or minus-end–directed movement during the course of the experiment revealed that over this 15 min time period nearly all mitochondria were motile (>95%). The fact that while nearly all mitochondria showed motility, only 57% were net displaced (Figure 3B) illustrates the bidirectional character of mitochondrial transport. Indeed, similar but opposing movements would offset each other, and a significant fraction of the mitochondria fell into this category (e.g., Figure 5C).

Surprisingly, expression of different PH domains had no effect on the total frequency of transport events (plus- and minus-end–directed combined). However, although in con-
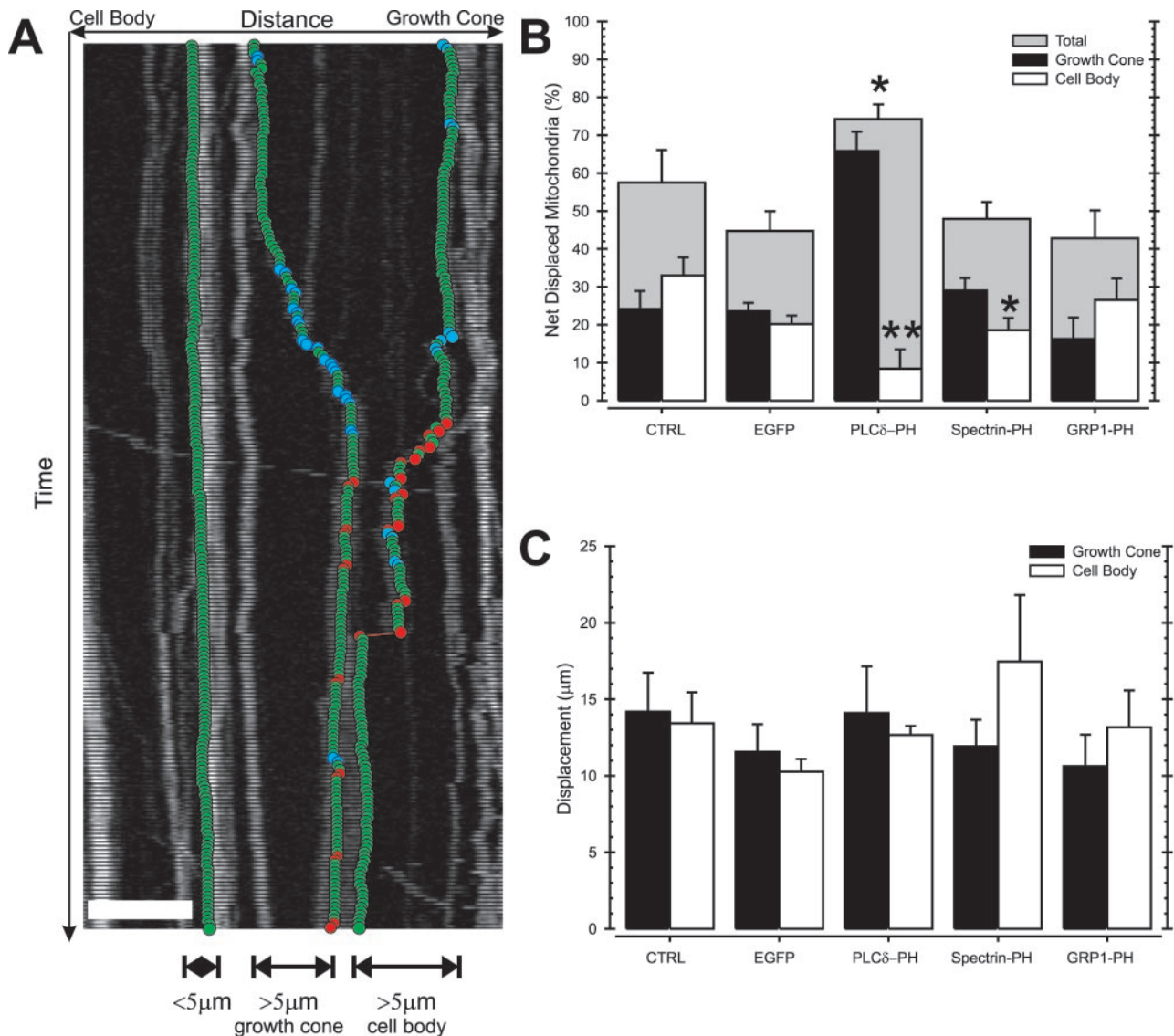
Figure 3. PtdIns(4,5)P2-specific PH domains enhance net mitochondrial transport toward the growth cone. N2A cells were transfected with DsRed1-Mito (CTRL), or cotransfected with DsRed1-Mito and EGFP (EGFP), EGFP-tagged PLCδ-PH (PLCδ-PH), spectrin-PH (Spectrin-PH), or GRP1-PH (GRP1-PH), and the position of axonal mitochondria was determined by fluorescence microscopy of DsRed1-Mito. As illustrated in A, the net displacement of mitochondria was defined as the absolute distance traveled during a 15-min period and obtained by comparing the start position and end position of each mitochondrion. The overall percentage of mitochondria that made a net displacement (threshold = 4 μm; gray filled bar) and the corresponding number of mitochondria that were net displaced toward the growth cone (black filled bar) or the cell body (open bar) are shown for the different treatments (B). The average growth cone (filled bar) and cell body-directed (open bar) net displacement was calculated by averaging of all recorded net displacements in the respective direction (C). Data shown are the mean and SEM of at least eight cells per condition and three independent experiments, *p < 0.05, **p < 0.01 (t test).

trol cells plus- and minus-end–directed transport events were balanced, PLCδ-PH expression enhanced the frequency of plus-end–directed movements twofold and at the same time reduced the frequency of minus-end–directed movements by half (Figure 4C). Similarly, spectrin-PH tilted the transport balance toward plus-end–directed mitochondrial transport. Neither EGFP nor GRP1-PH domain binding to 3′ phosphorylated PtdInsPs caused any change in transport (Figure 4C). Thus, PtdIns(4,5)P2-specific PH domains

modulated the balance between plus- and minus-end–directed transport of axonal mitochondria but not the overall frequency of transport events.

PtdIns(4,5)P2-specific PH Domains Diminish the Bidirectional Character of Mitochondrial Transport

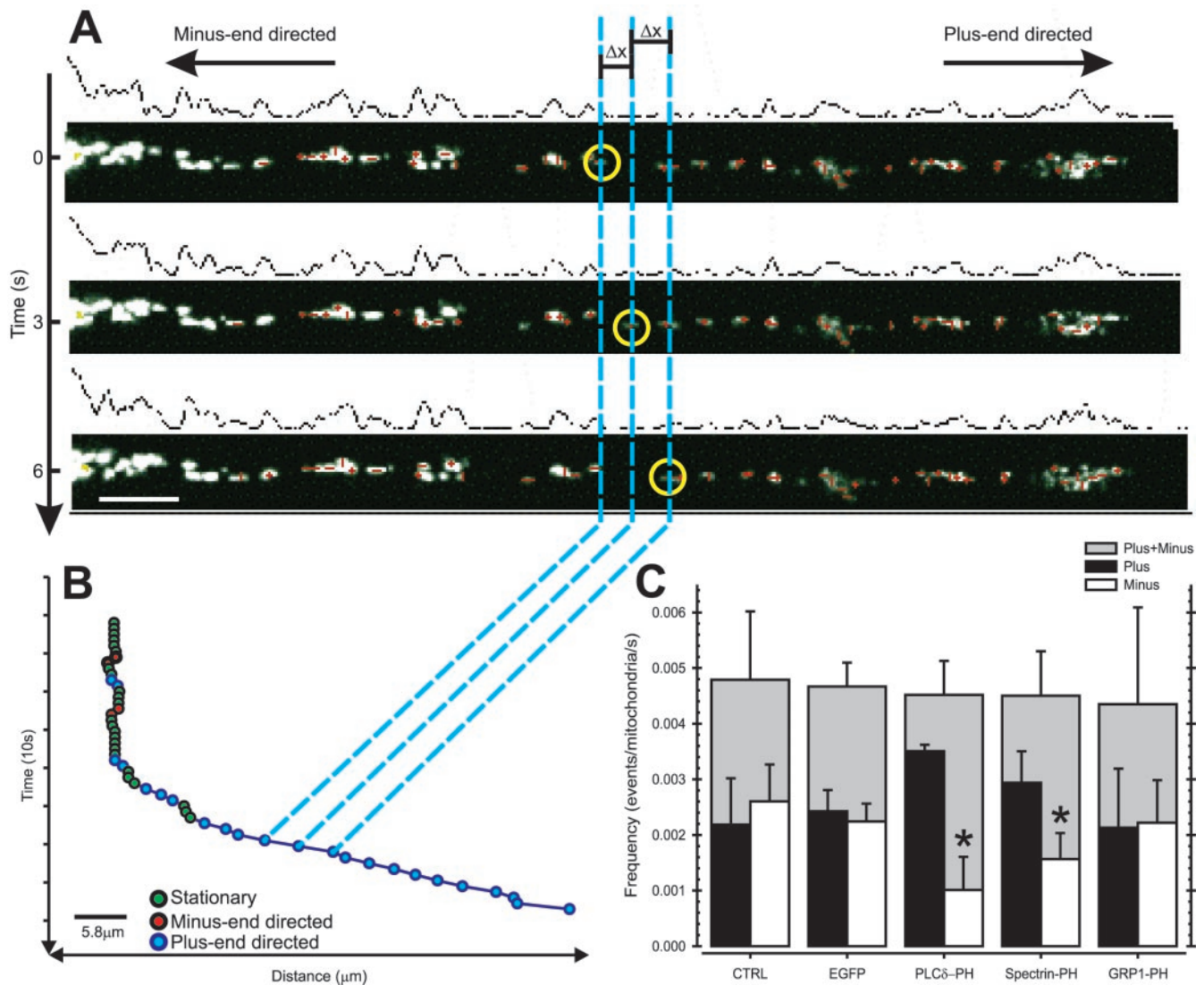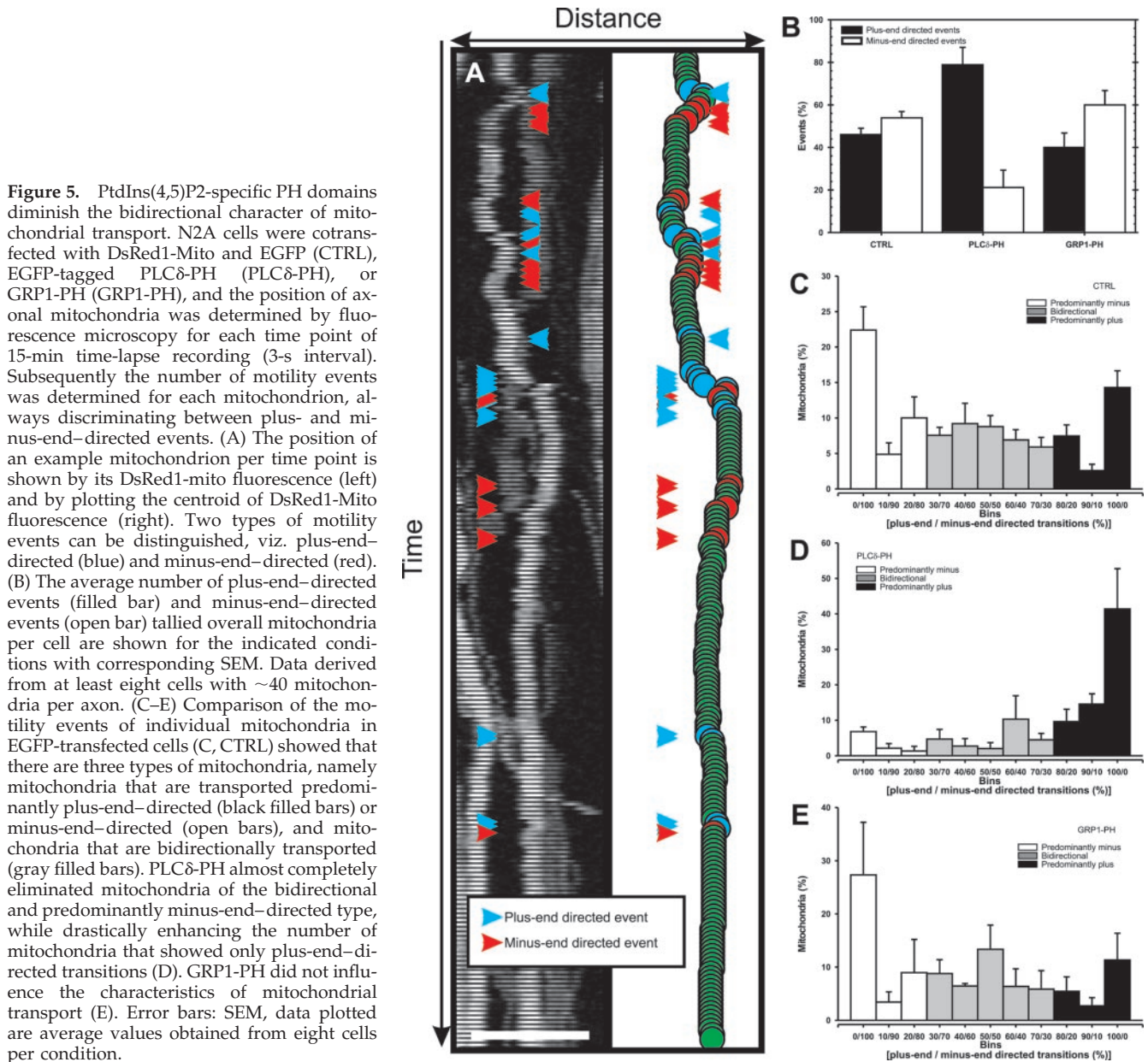We next characterized the transport behavior of individual mitochondria by analysis of the plus- and minus-end–

Figure 4. PtdIns(4,5)P2-specific PH domains modulate the balance between plus- and minus-end–directed MT-based transport of mitochondria. N2A cells were transfected with DsRed1-Mito (CTRL) or cotransfected with DsRed1-Mito and EGFP (EGFP), EGFP-tagged PLCδ-PH (PLCδ-PH), spectrin-PH (Spectrin-PH), or GRP1-PH (GRP1-PH). (A) The position of axonal mitochondria was recorded by time-lapse fluorescence microscopy of DsRed1-Mito and the centroid of fluorescence was determined for each mitochondrion per time point (A; red crosses). The frequency of mitochondrial movements was defined as the number of movement events above threshold ($\Delta x > 300$ nm/s) per axonal mitochondrion per second. Because of the highly organized MT-array in axons, directional information could be included. (B) The positions of an example mitochondrion (yellow circles in A) were plotted vs. elapsed time. Three types of events can be recognized, namely plus-end–directed motility events (blue), minus-end–directed motility events (red), and stationary periods (green). (C) The overall frequency of mitochondrial transport and SEM, viz. plus- and minus-end–directed transport combined (gray filled bar), and the corresponding plus- (black filled bar) and minus-end–directed (open bar) frequencies of mitochondrial movement and SEM are shown for the different treatments. Data shown are the mean and SEM of at least eight cells per condition and three independent experiments, *p < 0.05 (*t* test).

directed motility profile per mitochondria (see MATERIALS AND METHODS and Figure 5A). In control cells, the overall number of minus-end–directed motility events was equal to plus-end–directed events, as predicted from the net displacement and frequency data (Figure 5B). The motility histogram in Figure 5C shows that there were three types of motile mitochondria in the axons of control

cells, namely mitochondria that were transported predominantly in one direction, either minus- or plus-end–directed, and mitochondria that exhibited more balanced bidirectional transport. Forty-three percent of motile mitochondria exhibited bidirectional transport, whereas 32 and 23% were predominantly minus- and plus-end–directed, respectively.

Figure 5. PtdIns(4,5)P2-specific PH domains diminish the bidirectional character of mitochondrial transport. N2A cells were cotransfected with DsRed1-Mito and EGFP (CTRL), EGFP-tagged PLCδ-PH (PLCδ-PH), or GRP1-PH (GRP1-PH), and the position of axonal mitochondria was determined by fluorescence microscopy for each time point of 15-min time-lapse recording (3-s interval). Subsequently the number of motility events was determined for each mitochondrion, always discriminating between plus- and minus-end–directed events. (A) The position of an example mitochondrion per time point is shown by its DsRed1-mito fluorescence (left) and by plotting the centroid of DsRed1-Mito fluorescence (right). Two types of motility events can be distinguished, viz. plus-end–directed (blue) and minus-end–directed (red). (B) The average number of plus-end–directed events (filled bar) and minus-end–directed events (open bar) tallied overall mitochondria per cell are shown for the indicated conditions with corresponding SEM. Data derived from at least eight cells with ~40 mitochondria per axon. (C–E) Comparison of the motility events of individual mitochondria in EGFP-transfected cells (C, CTRL) showed that there are three types of mitochondria, namely mitochondria that are transported predominantly plus-end–directed (black filled bars) or minus-end–directed (open bars), and mitochondria that are bidirectionally transported (gray filled bars). PLCδ-PH almost completely eliminated mitochondria of the bidirectional and predominantly minus-end–directed type, while drastically enhancing the number of mitochondria that showed only plus-end–directed transitions (D). GRP1-PH did not influence the characteristics of mitochondrial transport (E). Error bars: SEM, data plotted are average values obtained from eight cells per condition.

In contrast, in PLCδ-PH–expressing cells, plus-end–directed events were markedly more abundant than minus-end–directed events (Figure 5B). Moreover, as shown in Figure 5D, we found that the majority of motile mitochondria made only plus-end–directed movements (74%). There were only 10% mitochondria that showed predominantly minus-end–directed motility and 16% were bidirectional. In GRP1-PH–expressing N2A cells, we observed a distribution similar to that in control cells, confirming that binding 3′ phosphorylated PtdInsPs did not alter the motility behavior of mitochondria (Figure 5, B and E). Thus, binding PtdIns(4,5)P2 efficiently eliminates minus-end–directed motility and disturbs the typical bidirectional behavior of most mitochondria.

Binding of PH Domains to PtdIns(4,5)P2 Does Not Affect Average Velocity and Duration of Mitochondrial Transport

To examine if PH domain binding to PtdIns(4,5)P2 affected the properties of mitochondrial motility in addition to the balance between plus- and minus-end–directed transport, we next accurately determined the velocity of mitochondrial transport, and the duration of unidirectional, continuous movements. Although the frequency of mitochondrial transport was an indicator of regulation of mitochondrial transport (activation vs. inactivation), both of these parameters described the physical properties of the molecular motors driving transport. The velocity is an indicator of the ATPase

Table 1. Velocity of mitochondrial movements in N2A axons

Treatment	Average velocity (μm/s)		Maximal velocity (μm/s)	
	Plus	Minus	Plus	Minus
CTRL	0.61 ± 0.024	0.67 ± 0.031	1.45 ± 0.07	1.44 ± 0.33
EGFP	0.59 ± 0.016	0.64 ± 0.025	1.36 ± 0.065	1.52 ± 0.069
PLCδ-PH	0.60 ± 0.13	0.69 ± 0.037	1.45 ± 0.041	1.59 ± 0.12
Spectrin-PH	0.61 ± 0.018	0.62 ± 0.026	1.38 ± 0.035	1.43 ± 0.050
GRP1-PH	0.62 ± 0.21	0.63 ± 0.02	1.44 ± 0.066	1.45 ± 0.039

Average velocities ± SEM were calculated for plus- and minus-end–directed mitochondrial movements in untransfected, EGFP, PLCδ-PH, spectrin-PH, and GRP1-PH–transfected cells by averaging all above threshold velocities (i.e., >300 nm/s). Maximal velocities ± SEM are the average of the 10% highest velocities recorded.

activity of the motor, whereas duration indicates the active period. The average velocity of plus- and minus-end–directed mitochondrial transport in control N2A cells were 0.61 μm/s and 0.67 μm/s, respectively (Table 1). These values were comparable to the reported velocities of mitochondria (Morris and Hollenbeck, 1995). Binding of PH domains to PtdIns(4,5)P2 or 3′ phosphorylated PtdInsPs did not affect the average velocity or maximal velocity of mitochondrial transport (Table 1).

The average duration of transport events was 3.9 and 4.3 s for plus- and minus-end–directed transport in control cells, with maximal durations of 9.8 and 11.3 s, respectively (Table 2). PH domain binding to PtdInsPs had no significant effect on the duration of mitochondrial transport (Table 2).

PtdIns(4,5)P2-specific PH Domains Do Not Influence Axonal Growth Rates

It has been reported that mitochondria accumulate in the vicinity of active, but not inactive growth cones (Morris and Hollenbeck, 1993). To investigate the possibility that the accumulation of mitochondria at the growth cone and the increase in plus-end–directed transport caused by PtdIns(4,5)P2-specific PH domains reflects axonal growth rate and growth cone activity, we determined the axonal growth rate of N2A axons for the different conditions. The average growth rate of control N2A axons was ~8 μm/h

(Table 3), which is comparable with values reported for DRGs and other neuronal cultures plated on poly-L-lysine (~10 μm/h; for overview see Gordon-Weeks, 2000). PH domain binding to PtdInsPs did not significantly influence the axonal growth rate (Table 3), thus excluding differences in axon outgrowth as an underlying cause for our observations.

PtdIns(4,5)P2-specific PH Domains Do Not Influence Binding of Molecular Motors to Mitochondria or MTs

One obvious mechanism by which PtdIns(4,5)P2-specific PH domains could influence transport of mitochondria is by modulation of the binding of molecular motors to mitochondria or MTs. Indeed, recent evidence suggests involvement of negatively charged PtdInsPs such as PtdIns(4,5)P2 in the binding of cytoplasmic dynein to brain vesicles in a spectrin-dependent way (Muresan *et al.,* 2001); and in the case of conventional kinesin, the alteration of kinesin-MT interactions affects regulation (Verhey *et al.,* 1998).

To investigate the association of molecular motors with mitochondria, we first determined the percentage of mitochondria that bound cytoplasmic dynein and kinesin by immunofluorescence. To avoid cytoplasmic background, we performed these experiments with mitochondria iso-

Table 2. Duration of mitochondrial movements in N2A axons

Treatment	Average duration (s)		Maximal duration (s)	
	Plus	Minus	Plus	Minus
CTRL	3.91 ± 0.26	4.28 ± 0.33	9.83 ± 0.61	11.30 ± 0.52
EGFP	3.90 ± 0.22	4.17 ± 0.31	9.91 ± 0.57	10.48 ± 0.48
PLCδ-PH	4.24 ± 0.48	4.77 ± 0.06	9.00 ± 0.53	12.38 ± 1.05
Spectrin-PH	4.80 ± 0.32	3.85 ± 0.27	12.45 ± 0.63	9.95 ± 1.03
GRP1-PH	3.86 ± 0.38	3.78 ± 0.35	12.16 ± 0.96	12.58 ± 1.42

Average durations ± SEM were calculated for plus- and minus-end–directed mitochondrial movements in untransfected (CTRL), EGFP, PLCδ-PH, spectrin-PH, and GRP1-PH–transfected cells by averaging all durations of events lasting at least 3 s (i.e., the time interval of recordings). Maximal durations ± SEM are the average of the 10% highest durations recorded. None of the durations was significantly different from control values.

Table 3. Average growth rate of N2A axons

Treatment	Average growth rate (μm/h)
CTRL	7.74 ± 0.73
EGFP	6.80 ± 1.26
PLCδ-PH	7.07 ± 1.42
Spectrin-PH	8.62 ± 1.36
GRP1-PH	9.62 ± 0.56

Average axonal growth rates ± SEM (n ≥ 5) were calculated for untransfected (CTRL) EGFP, PLCδ-PH, spectrin-PH, and GRP1-PH–transfected N2A cells plated on poly-L-lysine. Statistical analysis (*t*-test) revealed that there is no significant difference in growth rate for the different conditions compared with control.

lated from N2A cells expressing PH domains. Because we cotransfected PH domains with DsRed1-Mito, we were able to unambiguously distinguish mitochondria originating from transfected cells. Confocal microscopy showed that 35% of mitochondria from control-transfected cells stained positive for cytoplasmic dynein, whereas 45% stained positive for conventional kinesin (Figure 6, A and B). Neither PLCδ-PH nor spectrin-PH significantly changed the colocalization of cytoplasmic dynein or conventional kinesin with mitochondria. Similarly, GRP1-PH or EGFP expression did not affect attachment (Figure 6, A and B). This indicates that in the case of mitochondria, PtdInsPs are not required for retention of either molecular motor.

We confirmed these results by in vitro competition experiments. Isolated mitochondria from control cells were incubated with purified PtdInsP-binding PH domains and agents, and the amount of molecular motors bound was determined by Western blotting. As shown in Figure 6C, both cytoplasmic dynein and conventional kinesin were readily detected on isolated mitochondria. Binding PtdIns(4,5)P2 with purified PLCδ-PH, or the effector domain of MARCKS, a potent binder of negatively charged phospholipids (Taniguchi and Manenti, 1993; Kim *et al.*, 1994), did not alter the amount of molecular motors detected on mitochondria even while PLCδ-PH clearly bound to mitochondria (Figure 6C). Therefore, we concluded that the decrease in minus-end–directed transport elicited by PtdIns(4,5)P2-specific PH domains was not caused by reducing cytoplasmic dynein or increasing kinesin association with mitochondria.

Finally, we evaluated if PLCδ-PH modulated the affinity of molecular motors for MTs. We tested the binding of conventional kinesin and cytoplasmic dynein to MTs in the presence of AMP-PNP, a nonhydrolyzable ATP analog. The latter stabilized the motor-MT complex once formed. As was shown before, we found efficient binding of conventional kinesin and cytoplasmic dynein under control conditions (Figure 6D). Coincubation with PLCδ-PH did not alter the amount of molecular motors bound to MTs in this assay, excluding modulation of MT affinity as the underlying mechanism of the skewed mitochondrial transport in PLCδ-PH domain–expressing N2A cells.

DISCUSSION

In this study, we investigated the involvement of PtdInsPs in positioning of mitochondria in axons. We used differentiated N2A cells as a model for axonal transport. N2A cells are easily cultured and transfected in contrast to ex vivo neurons. N2A cells were used in previous studies of axonal organelle transport and localization (Ebneth *et al.*, 1998). It was shown before that N2A cells can extend axon-like processes (Ross *et al.*, 1975; Yu *et al.*, 1997). Under the conditions we used for differentiation, N2A cells put out axon-like processes that are positive for tau and negative for MAP2, as shown by immuno-staining with MAP2 and tau antibodies (supplementary Figure 1A). Transfection with PH domains did not change the nature of the processes (supplementary Figure 1B).

The amount of mitochondrial movements in N2A cells (0.47%) is lower than previously reported for bona fide neurons. This is at least in part due to the higher threshold (300 nm/s) used in this study to exclude any non–microtubule-based movements. Nevertheless, comparing axonal transport of mitochondria in N2A cells and dorsal root ganglions, we found similar characteristics (velocity and duration) although the overall level of motility was three- to fourfold lower in N2A cells (our unpublished results). Because the main observation of this study relates to the control of directionality of mitochondrial movements, but not the overall level of motility, we think that the N2A cells provide a useful model system.

We found that addition of the PH domains of either PLCδ1 or spectrin that bind PtdIns(4,5)P2 altered the distribution of mitochondria but not FM4−64 stained endosomes toward the growth cone (Figures 1 and 2, and supplementary Figure 2). Thus, PtdIns(4,5)P2-specific PH domains seem to specifically influence microtubule-based axonal transport of mitochondria. Interestingly, in CV1 fibroblasts we found no change in mitochondrial, endosome or lysosome distribution upon expression of PH domains indicating that PtdIns(4,5)P2-specific PH domains specifically target a neuron-specific pathway controlling mitochondrial distribution (supplementary Figure 3).

Analysis of the net displacement of individual mitochondria clearly showed that PH domain binding to PtdIns(4,5)P2 resulted in a larger number of mitochondria that were transported by microtubule motors toward the growth cone and a smaller number toward the cell body (Figure 3). In agreement with this observation, we found that binding PtdIns(4,5)P2 led to an increase in the frequency of plus-end–directed MT-based transport, which was accompanied by a drop in the minus-end–directed frequency (Figure 4). Furthermore, detailed analysis of the motile behavior of individual mitochondria in these cells showed that the majority of mitochondria were solely transported toward the growth cone without showing any minus-end–directed transport. In other words, the typical bidirectional transport of mitochondria was lost (Figure 5). Remarkably we did not find a change in the integrated frequency of MT-based transport (plus- and minus-end–directed frequency combined). Thus, binding PtdIns(4,5)P2 did not alter the overall level of mitochondrial transport but rather disturbed the balance between plus- and minus-end–directed transport.
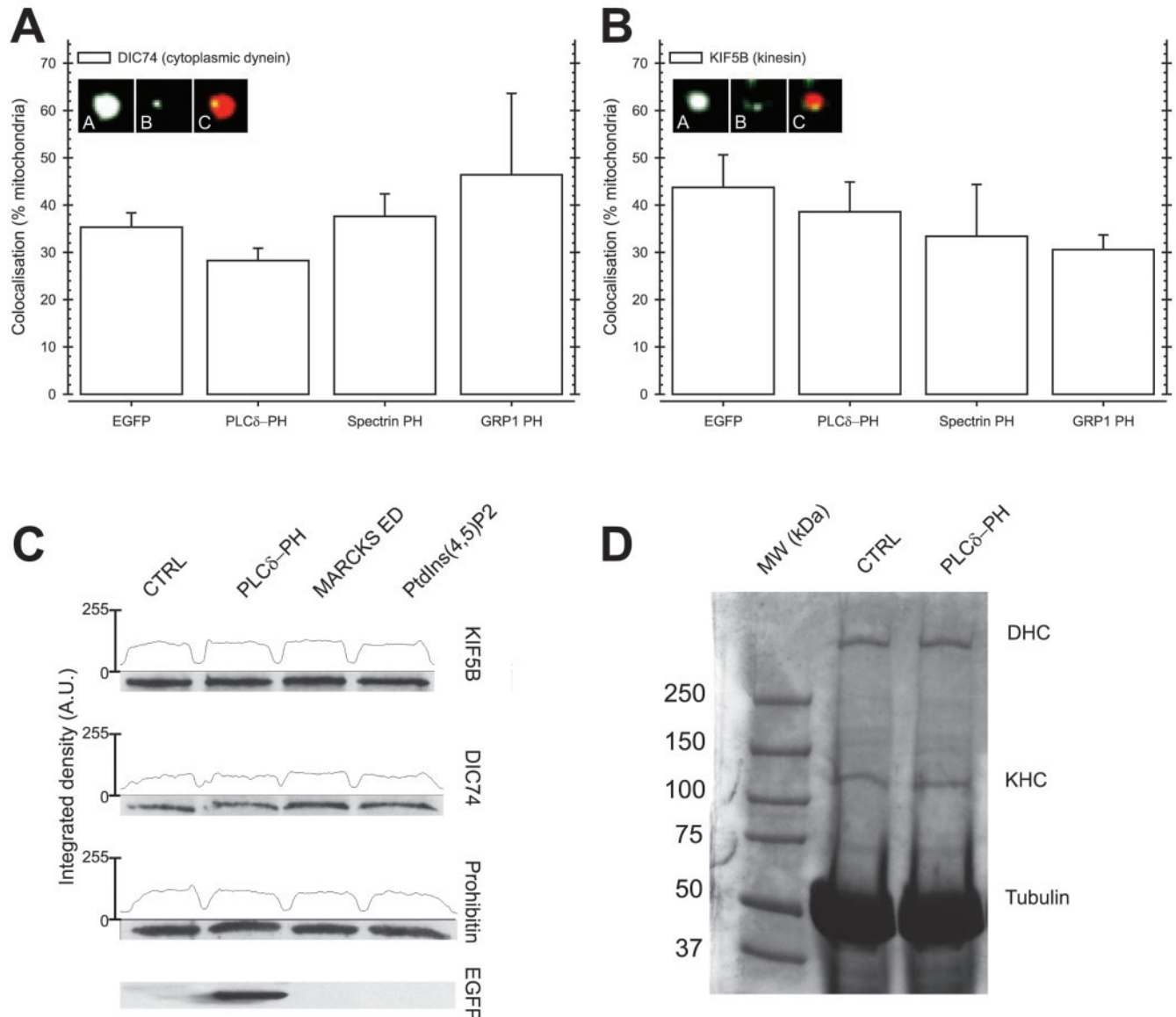
Figure 6. Binding of PtdIns(4,5)P2 or 3' phosphorylated PtdInsPs with PH domains does not influence interaction of molecular motors with mitochondria or MTs. (A and B) Mitochondria were isolated from N2A cells cotransfected with DsRed1-Mito and EGFP, PLCδ-PH, Spectrin-PH, or GRP1-PH. Colocalization of cytoplasmic dynein (A) and conventional kinesin (B) with mitochondria from transfected cells was determined by indirect immunofluorescence using antidynein IC 74 (DIC74) and antikinesin heavy chain (KIF5B) antibody, respectively. The results and SEM shown are derived from at least 200 DsRed1-Mito–positive mitochondria from three independent experiments. Representative mitochondria showing colocalization are shown as insets (a: mitochondrial DsRed1-mito fluorescence; b: DIC74 or KIF5B fluorescence; c: merge of a and b, colocalization shows up yellow). (C) Isolated mitochondria were incubated with purified PLCδ-PH, MARCKS effector domain peptide (MARCKS ED), or PtdIns(4,5)P2, and the amount of conventional kinesin (KIF5B) and cytoplasmic dynein (DIC74) was determined by Western blot analysis. As loading control, the amount of prohibitin, a mitochondrial marker protein, was determined in the same samples. Western blot detection of the EGFP-tag of PLCδ-PH showed significant amounts of PLCδ-PH bound to mitochondria (EGFP). (D) High-speed cytosol of untreated N2A cells was incubated with Taxol-stabilized MTs in the presence of AMP-PNP and purified PLCδ-PH. After separation on SDS-PAGE, MTs and MT-associated proteins were detected by Commassie-R250 staining. Clearly, the amount of cytoplasmic dynein heavy chain (DHC) and kinesin heavy chain (KHC) that bound to Taxol-stabilized MTs (Tubulin) after PLCδ-PH addition (PLCδ-PH) remained at control level (CTRL).

These observations suggest that there are two independent levels of regulation of mitochondrial transport in axons that govern mitochondrial distribution. First, there is regulation of the overall amount of mitochondrial transport, which is not dependent on free PtdIns(4,5)P2 concentration. Mitochondria are primarily stationary (99.5% of the time)

but can become motile (>95% of mitochondria did move in a 15-min period). Regulation of motility might involve docking of mitochondria to elements of the cytoskeleton such as intermediate filaments. Deletion of desmin from heart cells resulted in relocalization of mitochondria to the perinuclear region (Linden *et al.,* 2001), and redistribution of intermediate filaments upon heat shock correlated with perinuclear clustering of mitochondria (Collier *et al.,* 1993).

Second, once mitochondria are motile, there is regulation of the balance between mitochondrial transport toward the cell body and growth cone, which is, as shown here, clearly PtdIns(4,5)P2 dependent. Because we focused on MT-based transport of mitochondria and excluded actin-based transport based on velocity, the question becomes how does PtdIns(4,5)P2 regulate the balance between plus- and minus-end–directed MT-based transport of mitochondria? The parameters of vesicle motility that could be affected are 1) the velocity of movement, 2) the duration of movement, or 3) the control of directionality. Our observations show that the velocity and duration of mitochondrial transport are not affected by PtdIns(4,5)P2-binding PH domains. Velocity and duration of movement are properties of the motor and its environment, which suggests that the properties of the motors are not altered. In vitro studies suggest that negatively charged PtdInsPs sometimes mediate binding of molecular motors to vesicles (Muresan *et al.,* 2001; Klopfenstein *et al.,* 2002); however, we find that free PtdIns(4,5)P2 (or PtdIns(3,4,5)P3) is not required for binding of conventional kinesin or cytoplasmic dynein to mitochondria either in vivo or in vitro. In addition, the affinity of conventional kinesin or cytoplasmic dynein for MTs was not changed upon addition of PLCδ-PH. How then do PH domains influence mitochondrial motility? One possibility is that PH domains directly affect molecular motor activity. However, until now, we did not find any evidence supporting this possibility (unpublished data). Alternatively PH domains could interfere with signaling pathways that govern the activity of the molecular motors involved. These signaling pathways might emanate from the plasma membrane, where most of the cellular PtdIns(4,5)P2 is located; alternatively, direct binding of PH domains to mitochondria (Figure 6) might elicit effects on local, plasma membrane-independent signaling. One simple mechanism to explain these results is to suggest that a motor complex on the mitochondria surface has two controls, one for turning on motor activity and another for selecting which motor is active. In vitro reconstitution assays can test these possibilities. Known PtdIns(4,5)P2-dependent signaling pathways, such as activation of PKC, are currently under investigation.

In a previous review, we considered the problem of the balance of inward and outward movement, which is normally nearly equal (Hamm-Alvarez *et al.,* 1993). We suggested that for most cytoplasmic organelles, there is a normal cycle of outward and inward transport that is needed to explain the high level of vesicle transport normally observed (100s of fold greater than needed to explain synthesis and turnover; Sheetz, 1999). Unlike many other organelle systems, mitochondria have the ability to move in both directions at the any time in an axon or a localized region of cytoplasm. Thus, mitochondria can switch overall direction of transport at seemingly any time. What we observed here was that the switching of directions was particularly affected

by PH domain binding to PtdIns(4,5)P2. Our analysis of mitochondrial transport in axons suggests coordination of plus- and minus-end–directed transport of mitochondria. Binding PtdIns(4,5)P2 enhances plus-end–directed transport at the expense of minus-end–directed transport, almost eliminating bidirectional transport of mitochondria. Thus, there seems to be a feedback mechanism that coordinates molecular motors on the same organelle, so that only one motor gets activated even if there is a second motor present. A similar coordination was recently proposed (Gross *et al.,* 2002a; Gross *et al.,* 2002b).

The final distribution of an organelle within a cell is dependent on many factors in addition to motor activity; and coordination of different motors can be as important as the overall activity of the motors. In a typical cell, the amount of motility is much greater than is needed to move the organelles to their final destinations. Thus, the coordination of the two motors is critical and may well be the defining factor in determining the overall distribution in dynamic compartments.

Disruption of axonal transport of membranous organelles and mitochondria was implicated in neurodegenerative diseases such as Alzheimer's disease and amyotrophic lateral sclerosis (ALS; Torroja *et al.,* 1999; Kamal *et al.,* 2000; Gunawardena and Goldstein, 2001). Deregulation of cytoplasmic dynein-mediated, minus-end–directed transport was recently found to be sufficient to cause motor neuron degeneration such as that observed in ALS (LaMonte *et al.,* 2002), confirming earlier studies showing dramatic defects in axonal transport leading to a selective depletion of mitochondria in the degenerating axons of ALS patients (Collard *et al.,* 1995). Further evidence for a crucial role of mitochondrial transport in neural viability was proposed in models of ischemic delayed neuronal death, where immunohistochemical staining for cytoplasmic dynein and kinesin showed early and progressive decreases in molecular motor expression after ischemia coinciding with reductions of mitochondrial RNA levels and the activity of mitochondrial proteins (Abe *et al.,* 1995; Aoki *et al.,* 1995). Our finding that regulation of direction of mitochondrial transport in neurons is, at least in part, PtdIns(4,5)P2 dependent, suggests the interesting perspective that this regulatory mechanism might have implications in neurodegenerative diseases. Future studies will address this possibility.

ACKNOWLEDGMENTS

REFERENCES

Abe, K., Aoki, M., Kawagoe, J., Yoshida, T., Hattori, A., Kogure, K., and Itoyama, Y. (1995). Ischemic delayed neuronal death. A mitochondrial hypothesis. Stroke *26,* 1478–1489.

Aoki, M., Abe, K., Yoshida, T., Hattori, A., Kogure, K., and Itoyama, Y. (1995). Early immunohistochemical changes of microtubule based motor proteins in gerbil hippocampus after transient ischemia. Brain Res. *669,* 189–196.

Botelho, R.J., Teruel, M., Dierckman, R., Anderson, R., Wells, A., York, J.D., Meyer, T., and Grinstein, S. (2000). Localized biphasic changes in phosphatidylinositol-4, 5-bisphosphate at sites of phagocytosis. J. Cell. Biol. *151*, 1353–1368.

Bothmer, J., Markerink, M., and Jolles, J. (1992). Evidence for a new inositol phospholipid in rat brain mitochondria. Biochem. Biophys. Res. Commun. *187*, 1077–1082.

Brown, F.D., Rozelle, A.L., Yin, H.L., Balla, T., and Donaldson, J.G. (2001). Phosphatidylinositol 4, 5-bisphosphate and Arf6-regulated membrane traffic. J. Cell Biol. *154*, 1007–1017.

Collard, J.F., Cote, F., and Julien, J.P. (1995). Defective axonal transport in a transgenic mouse model of amyotrophic lateral sclerosis. Nature *375*, 61–64.

Collier, N.C., Sheetz, M.P., and Schlesinger, M.J. (1993). Concomitant changes in mitochondria and intermediate filaments during heat shock and recovery of chicken embryo fibroblasts. J. Cell Biochem. *52*, 297–307.

D'Andrea, L., Danon, M.A., Sgourdas, G.P., and Bonder, E.M. (1994). Identification of coelomocyte unconventional myosin and its association with in vivo particle/vesicle motility. J. Cell Sci. *107*, 2081–2094.

Davis, L.H., and Bennett, V. (1994). Identification of two regions of beta G spectrin that bind to distinct sites in brain membranes. J. Biol. Chem. *269*, 4409–4416.

De Vos, K., Severin, F., Van Herreweghe, F., Vancompernolle, K., Goossens, V., Hyman, A., and Grooten, J. (2000). Tumor necrosis factor induces hyperphosphorylation of kinesin light chain and inhibits kinesin-mediated transport of mitochondria. J. Cell Biol. *149*, 1207–1214.

Ebneth, A., Godemann, R., Stamer, K., Illenberger, S., Trinczek, B., and Mandelkow, E. (1998). Overexpression of tau protein inhibits kinesin-dependent trafficking of vesicles, mitochondria, and endoplasmic reticulum: implications for Alzheimer's disease. J. Cell Biol. *143*, 777–794.

Garcia, P., Gupta, R., Shah, S., Morris, A.J., Rudge, S.A., Scarlata, S., Petrova, V., McLaughlin, S., and Rebecchi, M.J. (1995). The pleckstrin homology domain of phospholipase C-delta 1 binds with high affinity to phosphatidylinositol 4, 5-bisphosphate in bilayer membranes. Biochemistry *34*, 16228–16234.

Gordon-Weeks, P.R. (2000). Neuronal Growth Cones. Cambridge, UK: Cambridge University Press.

Gross, S.P., Tuma, M.C., Deacon, S.W., Serpinskaya, A.S., Reilein, A.R., and Gelfand, V.I. (2002a). Interactions and regulation of molecular motors in Xenopus melanophores. J. Cell Biol. *156*, 855–865.

Gross, S.P., Welte, M.A., Block, S.M., and Wieschaus, E.F. (2002b). Coordination of opposite-polarity microtubule motors. J. Cell Biol. *156*, 715–724.

Gunawardena, S., and Goldstein, L.S. (2001). Disruption of axonal transport and neuronal viability by amyloid precursor protein mutations in Drosophila. Neuron *32*, 389–401.

Hamm-Alvarez, S.F., Kim, P.Y., and Sheetz, M.P. (1993). Regulation of vesicle transport in CV-1 cells and extracts. J. Cell Sci. *106*(Pt 3), 955–966.

Harlan, J.E., Hajduk, P.J., Yoon, H.S., and Fesik, S.W. (1994). Pleckstrin homology domains bind to phosphatidylinositol-4, 5-bisphosphate. Nature *371*, 168–170.

Helms, J.B., de Vries, K.J., and Wirtz, K.W. (1991). Synthesis of phosphatidylinositol 4, 5-bisphosphate in the endoplasmic reticulum of Chinese hamster ovary cells. J. Biol. Chem. *266*, 21368–21374.

Holz, R.W., Hlubek, M.D., Sorensen, S.D., Fisher, S.K., Balla, T., Ozaki, S., Prestwich, G.D., Stuenkel, E.L., and Bittner, M.A. (2000). A pleckstrin homology domain specific for phosphatidylinositol 4,

5-bisphosphate (PtdIns-4, 5-P2) and fused to green fluorescent protein identifies plasma membrane PtdIns-4, 5-P2 as being important in exocytosis. J. Biol. Chem. *275*, 17878–17885.

Ingold, A.L., Cohn, S.A., and Scholey, J.M. (1988). Inhibition of kinesin-driven microtubule motility by monoclonal antibodies to kinesin heavy chains. J. Cell Biol. *107*, 2657–2667.

Jellali, A., Metz-Boutigue, M.H., Surgucheva, I., Jancsik, V., Schwartz, C., Filliol, D., Gelfand, V.I., and Rendon, A. (1994). Structural and biochemical properties of kinesin heavy chain associated with rat brain mitochondria. Cell Motil. Cytoskel. *28*, 79–93.

Kamal, A., Stokin, G.B., Yang, Z., Xia, C.H., and Goldstein, L.S. (2000). Axonal transport of amyloid precursor protein is mediated by direct binding to the kinesin light chain subunit of kinesin-I. Neuron *28*, 449–459.

Kavran, J.M., Klein, D.E., Lee, A., Falasca, M., Isakoff, S.J., Skolnik, E.Y., and Lemmon, M.A. (1998). Specificity and promiscuity in phosphoinositide binding by pleckstrin homology domains. J. Biol. Chem. *273*, 30497–30508.

Khodjakov, A., Lizunova, E.M., Minin, A.A., Koonce, M.P., and Gyoeva, F.K. (1998). A specific light chain of kinesin associates with mitochondria in cultured cells. Mol. Biol. Cell *9*, 333–343.

Kim, J., Shishido, T., Jiang, X., Aderem, A., and McLaughlin, S. (1994). Phosphorylation, high ionic strength, and calmodulin reverse the binding of MARCKS to phospholipid vesicles. J. Biol. Chem. *269*, 28214–28219.

Klarlund, J.K., Tsiaras, W., Holik, J.J., Chawla, A., and Czech, M.P. (2000). Distinct polyphosphoinositide binding selectivities for pleckstrin homology domains of GRP1-like proteins based on diglycine versus triglycine motifs. J. Biol. Chem. *275*, 32816–32821.

Klopfenstein, D.R., Tomishige, M., Stuurman, N., and Vale, R.D. (2002). Role of phosphatidylinositol(4, 5)bisphosphate organization in membrane transport by the Unc104 kinesin motor. Cell *109*, 347–358.

Krendel, M., Sgourdas, G., and Bonder, E.M. (1998). Disassembly of actin filaments leads to increased rate and frequency of mitochondrial movement along microtubules. Cell Motil. Cytoskel. *40*, 368–378.

LaMonte, B.H., Wallace, K.E., Holloway, B.A., Shelly, S.S., Ascano, J., Tokito, M., Van Winkle, T., Howland, D.S., and Holzbaur, E.L. (2002). Disruption of dynein/dynactin inhibits axonal transport in motor neurons causing late-onset progressive degeneration. Neuron *34*, 715–727.

Leopold, P.L., McDowall, A.W., Pfister, K.K., Bloom, G.S., and Brady, S.T. (1992). Association of kinesin with characterized membrane-bounded organelles. Cell Motil. Cytoskel. *23*, 19–33.

Ligon, L.A., and Steward, O. (2000). Role of microtubules and actin filaments in the movement of mitochondria in the axons and dendrites of cultured hippocampal neurons. J. Comp. Neurol. *427*, 351–361.

Linden, M., Li, Z., Paulin, D., Gotow, T., and Leterrier, J.F. (2001). Effects of desmin gene knockout on mice heart mitochondria. J. Bioenerg. Biomembr. *33*, 333–341.

Milner, D.J., Mavroidis, M., Weisleder, N., and Capetanaki, Y. (2000). Desmin cytoskeleton linked to muscle mitochondrial distribution and respiratory function. J. Cell Biol. *150*, 1283–1298.

Morfini, G., Szebenyi, G., Elluru, R., Ratner, N., and Brady, S.T. (2002). Glycogen synthase kinase 3 phosphorylates kinesin light chains and negatively regulates kinesin-based motility. EMBO J. *21*, 281–293.

Morris, R.L., and Hollenbeck, P.J. (1993). The regulation of bidirectional mitochondrial transport is coordinated with axonal outgrowth. J. Cell Sci. *104*(Pt 3), 917–927.

Morris, R.L., and Hollenbeck, P.J. (1995). Axonal transport of mitochondria along microtubules and F-actin in living vertebrate neurons. J. Cell Biol. *131*, 1315–1326.

Muresan, V., Stankewich, M.C., Steffen, W., Morrow, J.S., Holzbaur, E.L., and Schnapp, B.J. (2001). Dynactin-dependent, dynein-driven vesicle transport in the absence of membrane proteins: a role for spectrin and acidic phospholipids. Mol. Cell *7*, 173–183.

Nangaku, M., Sato-Yoshitake, R., Okada, Y., Noda, Y., Takemura, R., Yamazaki, H., and Hirokawa, N. (1994). KIF1B, a novel microtubule plus end-directed monomeric motor protein for transport of mitochondria. Cell *79*, 1209–1220.

Rameh, L.E. *et al.* (1997). A comparative analysis of the phosphoinositide binding specificity of pleckstrin homology domains. J. Biol. Chem. *272*, 22059–22066.

Raucher, D., Stauffer, T., Chen, W., Shen, K., Guo, S., York, J.D., Sheetz, M.P., and Meyer, T. (2000). Phosphatidylinositol 4, 5-bisphosphate functions as a second messenger that regulates cytoskeleton-plasma membrane adhesion. Cell *100*, 221–228.

Rebecchi, M., Peterson, A., and McLaughlin, S. (1992). Phosphoinositide-specific phospholipase C-delta 1 binds with high affinity to phospholipid vesicles containing phosphatidylinositol 4, 5-bisphosphate. Biochemistry *31*, 12742–12747.

Reilein, A.R., Rogers, S.L., Tuma, M.C., and Gelfand, V.I. (2001). Regulation of molecular motor proteins. Int. Rev. Cytol. *204*, 179–238.

Reipert, S., Steinbock, F., Fischer, I., Bittner, R.E., Zeold, A., and Wiche, G. (1999). Association of mitochondria with plectin and desmin intermediate filaments in striated muscle. Exp. Cell Res. *252*, 479–491.

Rodionov, V.I., Gyoeva, F.K., Tanaka, E., Bershadsky, A.D., Vasiliev, J.M., and Gelfand, V.I. (1993). Microtubule-dependent control of cell shape and pseudopodial activity is inhibited by the antibody to kinesin motor domain. J. Cell Biol. *123*, 1811–1820.

Ross, J., Olmsted, J.B., and Rosenbaum, J.L. (1975). The ultrastructure of mouse neuroblastoma cells in tissue culture. Tissue Cell *7*, 107–135.

Seyfred, M.A., and Wells, W.W. (1984). Subcellular incorporation of 32P into phosphoinositides and other phospholipids in isolated hepatocytes. J. Biol. Chem. *259*, 7659–7665.

Sheetz, M.P. (1999). Motor and cargo interactions. Eur. J. Biochem. *262*, 19–25.

Stauffer, T.P., Ahn, S., and Meyer, T. (1998). Receptor-induced transient reduction in plasma membrane PtdIns(4, 5)P2 concentration monitored in living cells. Curr. Biol. *8*, 343–346.

Tanaka, Y., Kanai, Y., Okada, Y., Nonaka, S., Takeda, S., Harada, A., and Hirokawa, N. (1998). Targeted disruption of mouse conventional kinesin heavy chain, kif5B, results in abnormal perinuclear clustering of mitochondria. Cell *93*, 1147–1158.

Taniguchi, H., and Manenti, S. (1993). Interaction of myristoylated alanine-rich protein kinase C substrate (MARCKS) with membrane phospholipids. J. Biol. Chem. *268*, 9960–9963.

Toh, B.H., Lolait, S.J., Mathy, J.P., and Baum, R. (1980). Association of mitochondria with intermediate filaments and of polyribosomes with cytoplasmic actin. Cell Tissue Res. *211*, 163–169.

Torroja, L., Chu, H., Kotovsky, I., and White, K. (1999). Neuronal overexpression of APPL, the Drosophila homologue of the amyloid precursor protein (APP), disrupts axonal transport. Curr. Biol. *9*, 489–492.

Tran, D., Gascard, P., Berthon, B., Fukami, K., Takenawa, T., Giraud, F., and Claret, M. (1993). Cellular distribution of polyphosphoinositides in rat hepatocytes. Cell Signal. *5*, 565–581.

Vallis, Y., Wigge, P., Marks, B., Evans, P.R., and McMahon, H.T. (1999). Importance of the pleckstrin homology domain of dynamin in clathrin-mediated endocytosis. Curr. Biol. *9*, 257–260.

Verhey, K.J., Lizotte, D.L., Abramson, T., Barenboim, L., Schnapp, B.J., and Rapoport, T.A. (1998). Light chain-dependent regulation of Kinesin's interaction with microtubules. J. Cell Biol. *143*, 1053–1066.

Wang, T., Pentyala, S., Rebecchi, M.J., and Scarlata, S. (1999). Differential association of the pleckstrin homology domains of phospholipases C-beta 1, C-beta 2, and C-delta 1 with lipid bilayers and the beta gamma subunits of heterotrimeric G proteins. Biochemistry *38*, 1517–1524.

Watt, S.A., Kular, G., Fleming, I.N., Downes, C.P., and Lucocq, J.M. (2002). Subcellular localization of phosphatidylinositol 4, 5-bisphosphate using the pleckstrin homology domain of phospholipase C delta1. Biochem. J. *363*, 657–666.

Yu, W., Sharp, D.J., Kuriyama, R., Mallik, P., and Baas, P.W. (1997). Inhibition of a mitotic motor compromises the formation of dendrite-like processes from neuroblastoma cells. J. Cell Biol. *136*, 659–668.

Zagon, I.S., Higbee, R., Riederer, B.M., and Goodman, S.R. (1986). Spectrin subtypes in mammalian brain: an immunoelectron microscopic study. J. Neurosci. *6*, 2977–2986.